RSC Advances

PAPER

View Article Online
View Journal | View Issue

Cite this: *RSC Adv.*, 2015, **5**, 16190

Crystal structures, topologies and luminescent properties of three Zn(II)/Cd(II) coordination networks based on naphthalene-2,6-dicarboxylic acid and different bis(imidazole) linkers†

Zhi-Hao Yan,[ab] Wen Wang,[a] Liangliang Zhang,*[a] Xiaowei Zhang,[ab] Lei Wang,*[b] Rongming Wang[a] and Daofeng Sun[a]

Received 19th November 2014
Accepted 9th January 2015

DOI: 10.1039/c4ra14862b

www.rsc.org/advances

Three new mixed-ligand metal–organic coordination networks based on naphthalene-2,6-dicarboxylic acid and different bis(imidazole)s, $[Cd(bmimb)_{0.5}(ndc)]\cdot 1.5H_2O$ (**1**), $[Zn(bibp)(ndc)]\cdot H_2O$ (**2**), $[Zn(bip)(ndc)]\cdot 2H_2O$ (**3**), (bmimb = 1,4-bis((2-methyl-1*H*-imidazol-1-yl)methyl)benzene, bibp = 1,1′-(2,5-dimethyl-1,4-phenylene) bis(1*H*-imidazole), bip = 1,4-di(1*H*-imidazol-1-yl)benzene, H_2ndc = naphthalene-2,6-dicarboxylic acid), have been synthesized under solvothermal conditions and structurally characterized by single-crystal X-ray diffraction analyses, infrared spectroscopy (IR), elemental analyses, powder X-ray diffraction (PXRD) and thermogravimetric analyses (TGA). These complexes display different types of entanglements. Topological analysis reveals that **1** features a 3-fold interpenetrated **pcu** network constructed from paddle-wheel secondary building units. Complex **2** exhibits a normal mode of a 5-fold diamondoid interpenetrating net, while complex **3** is a 3D 4-connected coordination network with an extremely rare $(6^5\cdot 8)$-**hxg-d**-4-*Cccm* topology. These results suggest that both naphthalene-2,6-dicarboxylic acid and bis(imidazole) ancillary ligands influence the final resulting structures. Furthermore, luminescence properties and thermogravimetric properties of these complexes were investigated.

1. Introduction

Recently, the construction of coordination polymers (CPs) has attracted considerable attention not only for their potential applications in functional materials such as gas storage,[1] luminescence,[2] magnetism,[3] catalysis[4] and separation,[5] but also for their intriguing structural diversities and fascinating topological nets.[6] Although a lot of complexes have been reported, the rational and controllable preparation of coordination polymers remains an obvious challenge. To date, although a large number of entangled coordination polymers have been reported, it is difficult to identify the factors which play important roles in the formation of these structures. Many factors such as the metal ions, auxiliary N-donor ligands, reaction temperatures, pH values, and molar ratios of the components may contribute to the structural diversities.[7] It has been established that the design and choice of ligands are crucial for the construction of network topology.[8–10] Of all these, appropriate organic ligands are one of the most important factors because their length, steric effects, and flexibility will lead to diverse structures of coordination polymers.[11] Among various organic ligands, the aromatic multicarboxylate ligands play an important role in tuning the coordination framework structures owing to their abundant coordination modes to satisfy the geometric requirement of metal centers leading to fascinating structural architectures. Additionally, the presence of N-containing auxiliary ligands is also a rational and effective strategy for the fabrication of highly connected CPs. In this regard, various N-donor ligands are often employed to fabricate coordination polymers because of their excellent crystallinity and the relatively simple coordination geometries of the coordinated nitrogen atom(s). Hence the mixed-ligand system generated from polycarboxylic acids and N-donor ligands has been widely adopted for the assembly of new entangled coordination networks, which is endowed with abundant developed possibilities by the rational modulation of any component.

In this paper, we introduced two $-CH_3$ groups into the bis-imidazole to further investigate the substituted group impact on the structures of coordination polymers. It is noted that the spacer of these bis(imidazole) ligands (*e.g.* its length and conformation) sometimes plays a critical role on the final structure.

[a]*State Key Laboratory of Heavy Oil Processing, China University of Petroleum (East China), College of Science, China University of Petroleum (East China), Qingdao, Shandong 266580, P. R. China. E-mail: liangliangzhang@upc.edu.cn*

[b]*College of Chemistry and Molecular Engineering, Qingdao University of Science and Technology, Qingdao 266042, P. R. China. E-mail: inorchemwl@126.com*

† Electronic supplementary information (ESI) available: The preparation of complexes **1–3**, IR, PXRD patterns. CCDC 1028622–1028624. For ESI and crystallographic data in CIF or other electronic format see DOI: 10.1039/c4ra14862b

With the inspiration from the aforementioned points, the rigid linear dicarboxylate ligand and different bis(imidazole) auxiliary ligands were selected to construct new coordination polymers. Herein, we have successfully synthesized three mixed-ligand CPs under solvothermal conditions, namely, $[Cd(bmimb)_{0.5}(ndc)]\cdot 1.5H_2O$ (**1**), $[Zn(bibp)(ndc)]\cdot H_2O$ (**2**), $[Zn(bip)(ndc)]\cdot 2H_2O$ (**3**), (bmimb = 1,4-bis((2-methyl-1*H*-imidazol-1-yl)methyl)benzene, bibp = 1,1′-(2,5-dimethyl-1,4-phenylene)bis(1*H*-imidazole), bip = 1,4-di(1*H*-imidazol-1-yl) benzene, H_2ndc = naphthalene-2,6-dicarboxylic acid, Scheme 1). Three CPs vary their structures from 3D 3-fold interpenetrating **pcu** network and 3D **dia** to 6^3-**hcb** networks. Their syntheses, crystal structures, topologies, thermal stabilities and photoluminescent properties are reported in this paper.

2. Experimental

2.1. Materials and methods

Chemicals and solvents used in the syntheses were of analytical grade and used without further purification. IR spectra were measured on a Nicolet 330 FTIR Spectrometer at the range of 4000–400 cm^{-1}. Elemental analyses were carried out on a CE instruments EA 1110 elemental analyzer. Photoluminescence spectra were measured on a Hitachi F-7000 Fluorescence Spectrophotometer equipped (slit width: 5 nm; sensitivity: high). X-ray powder diffractions were measured on a Panalytical X-Pert pro diffractometer with Cu-Kα radiation. Thermogravimetric analyses were performed on a NETZSCH TG 209 F1 Iris® thermogravimetric analyser from 30 to 800 °C at a heating rate 10 °C min under the N_2 atmosphere (20 mL min^{-1}).

2.2. Synthesis of complexes 1–3

2.2.1. Synthesis of $[Cd(bmimb)_{0.5}(ndc)]\cdot 1.5H_2O$ (1). A mixture of $Cd(NO_3)_2\cdot 4H_2O$ (15 mg, 0.063 mmol), bmimb (5 mg, 0.019 mmol), H_2ndc (5.0 mg, 0.023 mmol) and 1.2 mL DMF–CH_3CN (v/v = 1 : 1) were sealed in a glass tube, and heated to 120 °C in 8 hours, kept 120 °C for 72 hours then slowly cooled to 30 °C in 13 hours. The colorless crystals were collected, washed with EtOH and dried in the air (yield: 80%). Elemental analysis calcd (%) for **1** ($C_{20}H_{15}CdN_2O_4$): C 52.25, H 3.29, N 6.09; found: C 50.85, H 2.91, N 5.91. Selected IR peaks (cm^{-1}): 3436 (s), 1707 (m), 1622 (s), 1515 (s), 1344 (s), 1076 (w), 1015 (w), 646 (w).

2.2.2. Synthesis of $[Zn(bibp)(ndc)]\cdot H_2O$ (2). A mixture of $Zn(NO_3)_2\cdot 6H_2O$ (11 mg, 0.037 mmol), bibp (5 mg, 0.021 mmol), H_2ndc (7.0 mg, 0.032 mmol) and 1.2 mL dioxane–H_2O (v/v = 1 : 1) were sealed in a glass tube, and heated to 120 °C in 8 hours, kept 120 °C for 72 hours then slowly cooled to 30 °C in 13 hours. The colorless crystals were collected, washed with EtOH and dried in the air (yield: 83%). Elemental analysis calcd (%) for 2 ($C_{26}H_{22}N_4O_5Zn$): C 58.28, H 4.14, N 10.46. Found: C 60.01, H. 4.56, N 9.95. Selected IR peaks (cm^{-1}): 3505 (s), 2953 (w), 2828 (w), 1639 (m), 1540 (m), 1493 (w), 1389 (w), 1240 (w), 1119 (s), 851 (w), 750 (w), 462 (w).

2.2.3. Synthesis of $[Zn(bip)(ndc)]\cdot 2H_2O$ (3). A mixture of $Zn(NO_3)_2\cdot 6H_2O$ (15 mg, 0.050 mmol), bip (5 mg, 0.024 mmol), H_2ndc (7.0 mg, 0.032 mmol), KOH (0.1 M, 0.05 mL) and 1.2 mL DMF–NMP–H_2O (v/v/v = 1 : 1 : 1) were sealed in a glass tube, and heated to 120 °C in 8 hours, kept 120 °C for 67 hours then slowly cooled to 30 °C in 13 hours. Colorless crystals of **3** were obtained in 61% yield based on Zn. Elemental analysis calcd (%) for **3** ($C_{48}H_{28}N_8O_9Zn_2$): C 58.14, H 2.85, N 11.30. Found: C 60.06, H. 2.45, N 12.42. Selected IR peaks (cm^{-1}): 3489 (w), 1605 (m), 1530 (s), 1492 (s), 1433 (s), 1401 (s), 1238 (s), 1206 (m), 1120 (s), 1018 (m), 845 (m), 750 (s), 584 (m), 537 (w), 490 (w).

2.3. X-ray crystallography

Single crystals of the complexes **1–3** with appropriate dimensions were chosen under an optical microscope and quickly coated with high vacuum grease (Dow Corning Corporation) before being mounted on a glass fiber for data collection. Data for them were collected with a SuperNova CCD diffractometer with graphite-monochromated Mo Kα radiation source (λ = 0.71073 Å), and there was no evidence of crystal decay during data collection. A preliminary orientation matrix and unit cell parameters were determined from 3 runs of 12 frames each, each frame corresponds to a 0.5° scan in 5 s, followed by spot integration and least-squares refinement. For **1–3**, data were measured using scans of 0.5° per frame for 10 s until a complete hemisphere had been collected. Cell parameters were retrieved using SMART software and refined with SAINT on all observed reflections.[12] Data reduction was performed with the SAINT software and corrected for Lorentz and polarization effects. Absorption corrections were applied with the program SADABS.[12] In all cases, the highest symmetry was chosen. All structures were solved by direct methods using SHELXS-97 (ref. 13) and refined on F^2 by full-matrix least-squares procedures with SHELXL-97.[14] Atoms were located from iterative examination of difference *F*-maps following least squares refinements of the earlier models. Hydrogen atoms were placed in calculated positions and included as riding atoms with isotropic displacement parameters 1.2–1.5 times U_{eq} of the attached C atoms. All structures were examined using the Addsym subroutine of PLATON[15] to assure that no additional symmetry could be applied to the models. Pertinent crystallographic data collection

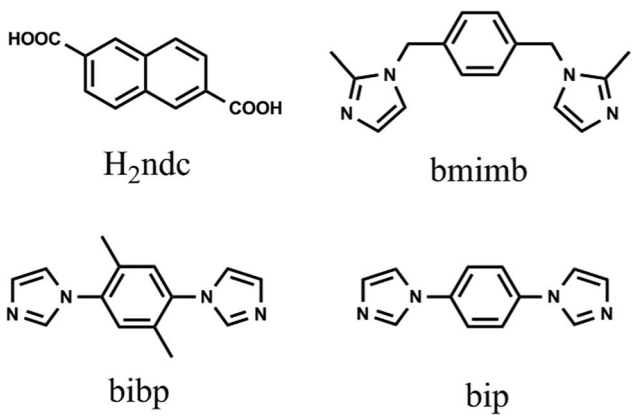

Scheme 1 Structures of H_2tbtpa and N-donor ligands used in this work.

Table 1 Crystal data for **1–3**[a]

Complex	**1**	**2**	**3**
Empirical formula	$C_{20}H_{15}N_2O_4Cd$	$C_{26}H_{22}N_4O_5Zn$	$C_{48}H_{28}N_8O_9Zn_2$
Formula weight	459.74	535.85	991.52
Temperature/K	295.45(10)	296.11(13)	297.78(10)
Crystal system	Triclinic	Triclinic	Monoclinic
Space group	$P\bar{1}$	$P\bar{1}$	$C2/c$
a/Å	8.3360(5)	9.5458(3)	22.7709(6)
b/Å	10.5155(6)	10.5524(3)	11.0788(2)
c/Å	13.4550(8)	13.9153(5)	18.5004(6)
α/°	105.088(5)	70.299(3)	90.00
β/°	107.870(5)	79.799(3)	105.721(3)
γ/°	90.637(5)	72.102(3)	90.00
Volume/Å^3	1078.51(11)	1251.56(8)	4492.6(2)
Z	2	2	4
ρ_{calc} mg mm^{-3}	1.416	1.422	1.466
μ/mm^{-1}	1.036	1.025	1.134
F(000)	458.0	552.0	2016.0
Index ranges	$-9 \le h \le 9$, $-12 \le k \le 12$, $-15 \le l \le 16$	$-11 \le h \le 11$, $-11 \le k \le 12$, $-16 \le l \le 16$	$-25 \le h \le 27$, $-13 \le k \le 6$, $-22 \le l \le 18$
Reflections collected	8831	12 593	7483
Independent reflections	3780 [R(int) = 0.0279]	4409 [R(int) = 0.0479]	3995 [R(int) = 0.0264]
Data/restraints/parameters	3780/0/245	4409/0/330	3995/114/351
Goodness-of-fit on F^2	1.182	1.081	1.032
Final R indexes [$I \ge 2\sigma(I)$]	$R_1 = 0.0400$, w$R_2 = 0.1288$	$R_1 = 0.0745$, w$R_2 = 0.2226$	$R_1 = 0.0486$, w$R_2 = 0.1353$
Final R indexes [all data]	$R_1 = 0.0437$, w$R_2 = 0.1333$	$R_1 = 0.0820$, w$R_2 = 0.2308$	$R_1 = 0.0587$, w$R_2 = 0.1443$
Largest diff. Peak/hole/e Å^{-3}	1.94/−0.47	1.55/−0.59	0.76/−0.65

[a] $R_1 = \Sigma||F_o| - |F_c||/\Sigma|F_o|$, w$R_2 = [\Sigma w(F_o^2 - F_c^2)^2]/\Sigma w(F_o^2)^2]^{1/2}$.

and refinement parameters are collated in Table 1. Selected bond lengths and angles are collated in Table 2.

3. Result and discussion

3.1. Synthesis and general characterization

All crystallization of complexes **1–3** were obtained under similar reaction conditions by solvothermal methods, by changing metal ions and solvent, the crystals suitable for the single-crystal X-ray diffraction analysis were finally obtained after cooling to room temperature. All complexes are stable in the solid state upon extended exposure to air and they have poor solubility in common organic solvents and only are slightly soluble in a very high polarity solvents, such as DMF, DEF, and DMSO.

Powder X-ray diffraction (PXRD) has been used to check the phase purity of the bulk samples in the solid state. For complexes **1–3**, the measured PXRD patterns closely match the simulated patterns generated from the results of single-crystal diffraction data (Fig. S1, ESI†), indicative of pure products.

Table 2 Selected bond lengths (Å) and angles (°) for **1–3**

Complex 1							
Cd1–O1	2.258(4)	Cd1–O2	2.247(4)	Cd1–O3	2.222(4)	Cd1–O4	2.227(4)
Cd1–N1	2.214(5)						
O4–Cd1–O2	90.45(16)	O4–Cd1–O1	88.58(17)	O3–Cd1–O4	156.07(18)	O3–Cd1–O2	86.31(17)
O3–Cd1–O1	84.95(18)	O2–Cd1–O1	156.03(18)	N1–Cd1–O4	95.79(17)	N1–Cd1–O3	108.09(18)
N1–Cd1–O2	101.76(17)	N1–Cd1–O1	102.17(17)				
Symmetry codes: (i): $-x$, $1-y$, $-z$; (ii): $2-x$, $2-y$, $1-z$; (iii): $-x$, $1-y$, $1-z$; (iv): $1-x$, $-y$, $-z$							
Complex 2							
Zn1–O1	1.964(4)	Zn1–O3	1.971(4)	Zn1–N1	2.043(4)	Zn1–N3	2.008(4)
O1–Zn1–O3	107.29(19)	O1–Zn1–N3	116.31(19)	O1–Zn1–N1	96.08(18)	O3–Zn1–N1	114.00(17)
O3–Zn1–N3	117.52(18)	N3–Zn1–N1	103.71(16)				
Symmetry codes: (i): $1-x$, $-1-y$, $2-z$; (ii): $-x$, $-y$, $1-z$; (iii): $-x$, $1-y$, $2-z$; (iv): $2-x$, $1-y$, $1-z$							
Complex 3							
Zn1–O1	1.947(2)	Zn1–O3	1.957(2)	Zn1–N1	2.037(3)	Zn1–N3^i	2.009(2)
O1–Zn1–O3	118.70(11)	O1–Zn1–N1	108.70(11)	O1–Zn1–N3^i	101.27(10)	O3–Zn1–N1	103.05(13)
O3–Zn1–N3^i	120.19(12)	N3^i–Zn1–N1	103.75(10)				
Symmetry codes: (i): $-1/2+x$, $1/2-y$, $-1/2+z$; (ii): $1/2-x$, $3/2-y$, $-z$; (iii): $1-x$, $-y$, $-z$; (iv): $1/2+x$, $1/2-y$, $1/2+z$							

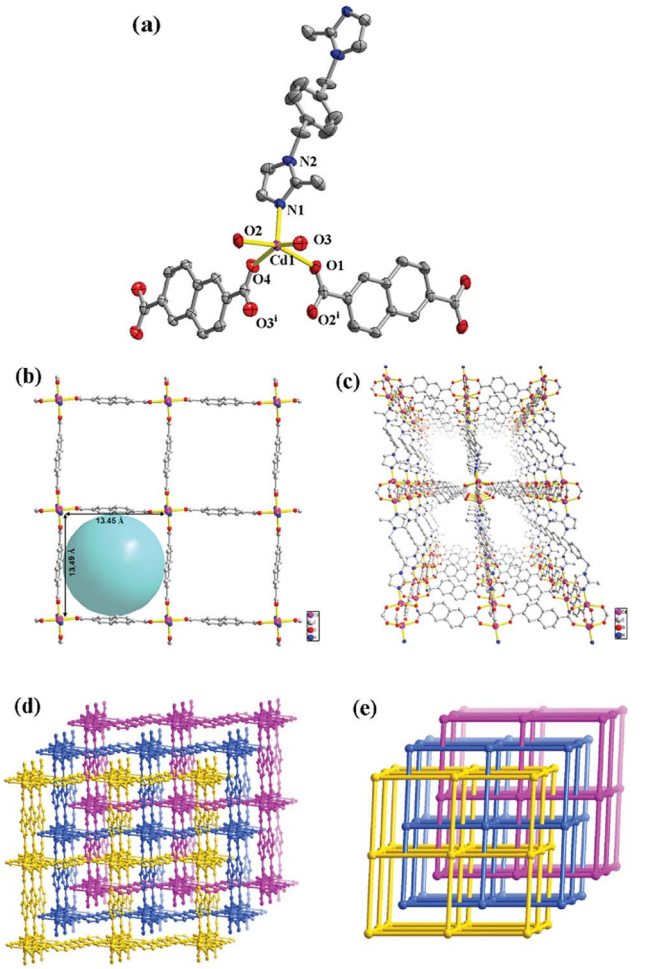

Fig. 1 (a) Coordination environment of the Cd(II) cation in **1**. (Symmetry codes: (i): $-x, 1-y, -z$; (ii): $2-x, 2-y, 1-z$; (iii): $-x, 1-y, 1-z$; (iv): $1-x, -y, -z$); (b) 2D flat network with square grids constructed by ndc ligands and Cd(II) ions in **1**. (c) Schematic illustrating a single 3D framework pillared by bmimb ligands. 3D framework of **1**. (d) The 3-fold interpenetrating 3D framework. (e) The 3D network with **pcu** topology for **1**.

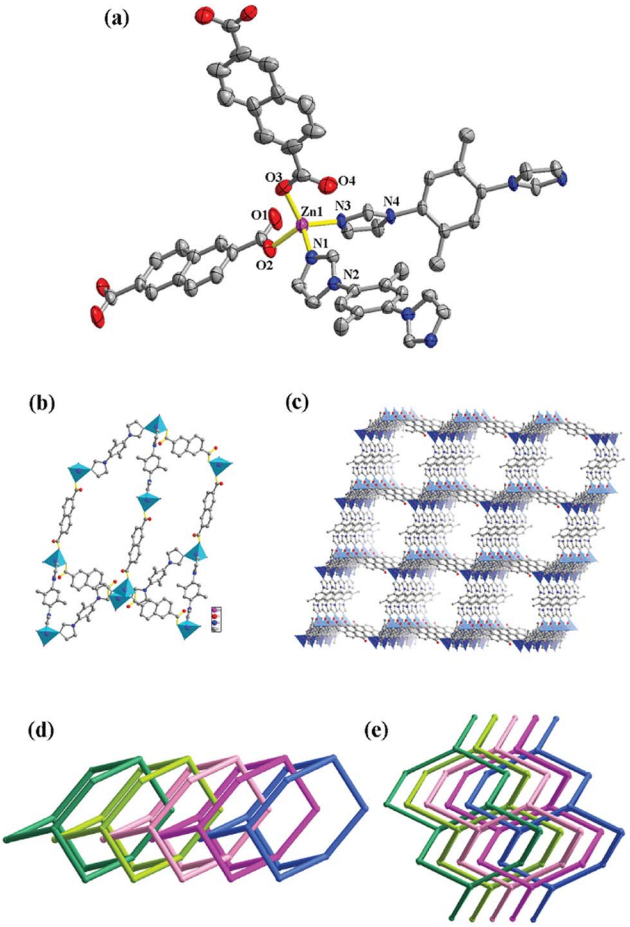

Fig. 2 (a) Coordination environment of the Zn(II) cation in **2**. (Symmetry codes: (i): $1-x, -1-y, 2-z$; (ii): $-x, -y, 1-z$; (iii): $-x, 1-y, 2-z$; (iv): $2-x, 1-y, 1-z$). (b) View of the superadamantane. (c) Schematic illustrating the 3D framework of **2**. (d) Schematic representation of the 5-fold interpenetrating network. (e) The 5-fold interpenetrating framework with **dia** topology.

The IR spectra (Fig. S2, ESI†) of complexes **1–3** also show characteristic absorption bands mainly attributed to the asymmetric (ν_{as}: *ca.* 1600 cm^{-1}) and symmetric (ν_s: *ca.* 1385 cm^{-1}) stretching vibrations of the carboxylate groups. No band in the region 1690–1730 cm^{-1}, indicates complete deprotonation of the carboxylic groups,[16] which is consistent with the result of the X-ray diffraction analysis.

3.2. Structure descriptions

3.2.1. $[Cd(bmimb)_{0.5}(ndc)]\cdot 1.5H_2O$ (1). Single crystal X-ray diffraction analysis reveal that complex **1** with a pillared structure was obtained. It exhibits a 3-fold interpenetrated 3D framework with the classic **pcu** topology, and the asymmetric unit consists of one Cd(II) ion, two halves of ndc ligands, and one half the bmimb ligand. As shown in Fig. 1a, the crystallographically unique Cd(II) atom has a square pyramidal coordination geometry ($\tau_5 = 0.007$)[17] surrounded by four oxygen atoms [Cd–O = 2.222(4)–2.258(4) Å] from different ndc ligands in the equatorial plane and a nitrogen atom [Cd–N(apical), 2.214(5) Å] from a bmimb ligand at the axial position. As illustrated in Fig. 1b, two adjacent crystallographically equivalent Cd(II) atoms are connected by two pairs of carboxylates to form a paddle-wheel shaped $[Cd_2(CO_2)_4]$ dimer with a Cd(II)···Cd(II) distance of 3.1476(7) Å, which is in the normal range observed for other $[M_2(CO_2)_4]$ paddle-wheel units.[18] Each dinuclear unit has a crystallographic inversion center at the center of Cd–Cd cores, and the $[Cd_2(CO_2)_4]$ subunit is bonded to four identical dimeric units through four bridging ndc ligands to afford an extended 2D square-grid (4,4) layer with large grid windows of 13.455×13.4912 $Å^2$ in dimension. These 2D sheets are further connected together in the third dimension by axially coordinating bmimb ligands to give a 3D open framework (Fig. 1c) that possesses largely distorted cubelike cavities approximately $13.46 \times 13.49 \times 18.82$ $Å^3$ in size.

From the topological view, the $[Cd_2(CO_2)_4]$ dimer can be simplified as a six-connected node, the pillared bmimb ligands are taken as linkers and the 3D structure can be classified as a

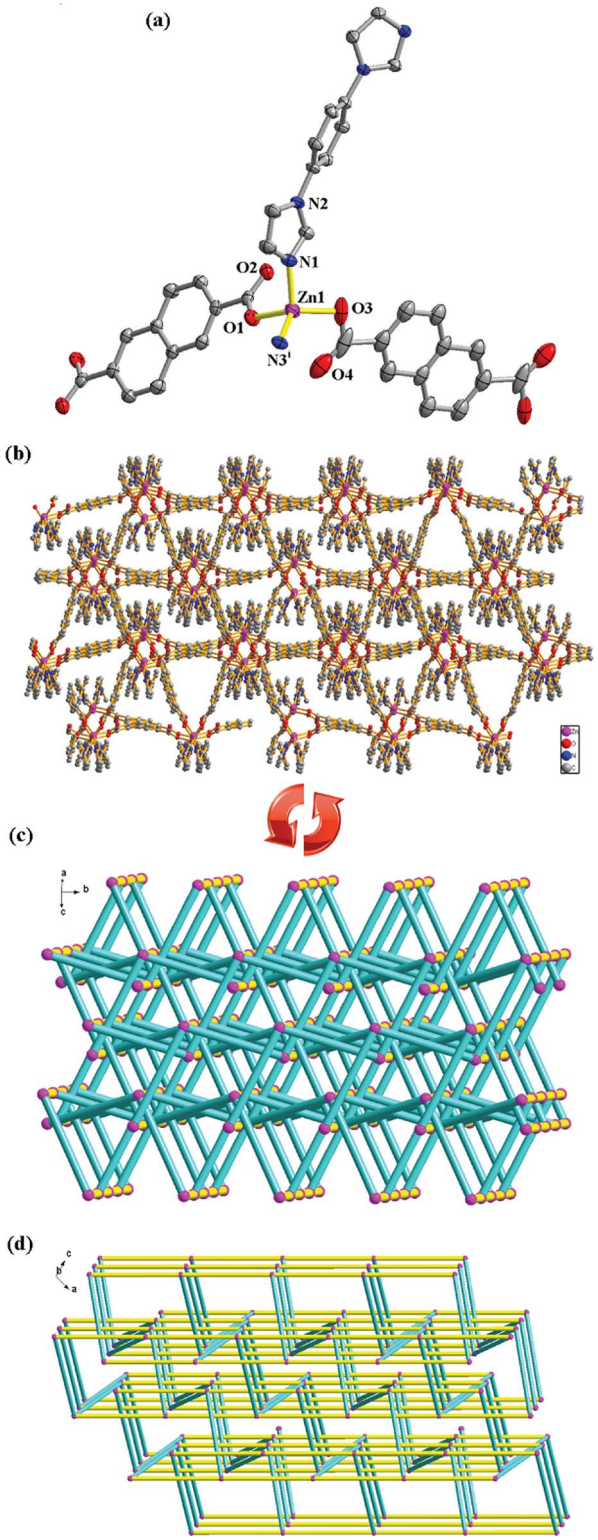

Fig. 3 (a) Coordination environment of the Zn(II) cation in **3**. (Symmetry codes: (i): −1/2 + *x*, 1/2 − *y*, −1/2 + *z*; (ii): 1/2 − *x*, 3/2 − *y*, −*z*; (iii): 1 − *x*, −*y*, −*z*; (iv): 1/2 + *x*, 1/2 − *y*, 1/2 + *z*). (b) Ball-and-stick representation of the 3D framework (purple ball, Zn; blue ball, N; red ball, O; gray ball, C). (c) The 3D framework with the $(6^5\cdot 8)$-**hxg-d**-4-*Cccm* topology. (d) The topological representation of **3** along the *b* axis.

classical **pcu** architecture (α-topology).[19] Of particular interest, this large super framework gives the single **pcu** network a huge chamber which allows the other two identical 3D single frameworks to penetrate, thus giving a 3-fold interpenetrated 3D to 3D framework (Fig. 1d and e). Furthermore, a close inspection of the porous complex discloses that there is one type of rhombic channel.

3.2.2. [Zn(bibp) (ndc)]·H_2O (2). When the auxiliary ligand was changed from semiflexible bmimb to rigid bibp used in the preparation for **2**. We obtained complex **2** as a 5-fold interpenetrated 3D framework with a typically diamond topology. Single crystal X-ray analysis reveals that **2** crystallized in a triclinic space group of $P\bar{1}$. As shown in Fig. 2a, the asymmetric unit of **2** consists of one crystallographically independent Zn(II) ion, two halves of bibp, two halves of ndc ligands and one guest water molecule. The coordination geometry of the Zn(II) cation adopts a distorted tetrahedron geometry defined by four atoms, including two carboxylic oxygen atoms [Zn–O1 = 1.964(4) Å, Zn–O3 = 1.971(4) Å] from two different ndc ligands and two nitrogen atoms [Zn–N1 = 2.043(4) Å, Zn–N3 = 2.008(4) Å] from two bibp ligands, the Zn–O/N bond distances fall in the normal range found in other Zn complexes.[20] The bond angles for Zn are in the range of 96.09(18)–117.53(18), with an average value of 109.15(10), which slightly deviates from an angle of 109.47 in a perfect tetrahedron. And the distortion of the tetrahedron can be indicated by the calculated value of the τ_4 parameter introduced by Houser[21] to describe the geometry of a four-coordinate metal system, which is 0.89 for Zn (for an ideal tetrahedron $\tau_4 = 1$).

A better insight into the nature of **2** can be provided by a topology analysis. The extension of the structure of **2** into a 3D network is accomplished by binding two μ_2-bibp and two μ_2-η_1,η_1-ndc ligands to the four-connected Zn(II) nodes. The topological analysis of **2** reveals that it is a typically diamondoid framework containing large cages consists of $[Zn_{10}(bibp)_6(ndc)_6]$ adamantane-liked subunits. A single adamantanoid framework is illustrated in Fig. 2b, which possesses maximum dimensions (the longest intracage distances across the unit along the directions) of 33.32 × 22.29 × 26.77 $Å^3$. Because of the spacious nature of the single network, it allows another four identical diamondoid networks to interpenetrate it in a normal mode giving rise to a 5-fold interpenetrating **dia** array (Fig. 2d and e), with isolated water molecules occupying the neutral channels. As we known, many 3D nets with diamond topology of various interpenetration degrees ranging from 2- to 11-fold have been reported, 5-fold interpenetrating CPs in the presence of mixed ligands with different lengths are relatively common.[22]

3.2.3. [Zn(bip)(ndc)]·$2H_2O$ (3). When the rigid ligand without –CH_3 groups was introduced in the preparation for **3**, a new 4-connected net was obtained. The single-crystal diffraction analysis indicates that complex **3** crystallized in a monoclinic manner with space group *C*2/*c*. The asymmetric unit of **3** consists of one independent Zn(II) ion, one bip ligand, two halves of ndc ligands and one guest water molecule. The Zn(II) center is situated in distorted tetrahedron geometry. As depicted in Fig. 3a, Zn1 is four-coordinated by two nitrogen atoms

[Zn–N1 = 2.037(3) Å, Zn–N3^{i} = 2.009(2) Å] from two bip ligands and two oxygen atoms [Zn–O1 = 1.947(2) Å, Zn–O3 = 1.957(2) Å] from two ndc anions in a distorted tetrahedral coordination environment. The τ_4 parameter is 0.94 for Zn1. The nitrogen atoms of the bip ligands link the Zn(II) cation centers into an infinite 1D zig-zag chain, which contains a Zn⋯Zn separation of 12.575(2) Å (Fig. S3, ESI†). Such 1D zig-zag chains are further linked by the ndc ligands, leading to the formation of a 3D framework without interpenetration possessing large channels along the *b* direction (Fig. 1b). It is obvious that the presence of the large voids in **3** facilitates the residing of H_2O inside the framework.

From the view of topology, by treating the Zn(II) atom as a single node and connecting the nodes according to the connectivity defined by ndc and bip ligands. Hence the 3D network has the Wells point symbol Schläfli symbol of $(6^5\cdot 8)$, so this 3D net could be simplified to a 4-connected uninodal net of **hxg**-d-4-*Cccm* topology (Fig. 1c) with the vertex symbol of {6.6.6.6.6(2).10(12)}.

It should be mentioned that the **hxg-d** network topology is different from the known, but rarely reported, 6-connected $(4^6\cdot 6^9)$ **hxg** net.[23] A detailed comparison of the two nets (**hxg-d** *vs.* **hxg**) is discussed below. For each periodic network, there is a unique 'natural' tiling.[24] The **hxg-d** net has the natural tiling $[4^6]$, whereas the tile $[4^6\cdot 6^4]$ is found for the **hxg** net. The Zn as a tiling is derived by placing a new vertex inside each tile and connecting pairs of new vertices which are in adjacent tiles by a new edge through the face common to another tile.[25]

3.3. The influence of metal center and N-donor ligand on the structures

As discussed above, it was evident that the coordination geometries of the central metal ions and the coordination modes of the organic ligands have an effect on the formation and dimensions of the final structures. And it is most interesting to note that the bis(imidazole) spacers play important roles in directing the final structures of complexes **1–3**. Here, three kinds of N-donor (bmimb, bibp, bip) bridging ligands were used as secondary ligands to investigate their effects on the structure and topology of the resulting frameworks **1–3**. In complex **1** the Cd(II) center acts as a 5-connected node, whereas in **2** and **3** the Zn(II) centers are 4-connected by the ndc dianion and rigid bis(imidazole) ligand. In **1–3**, although all bis(imidazole) auxiliary ligands adopts similar μ_2 bridging coordination modes, their spatial orientations are quite different, which result in variable topologies of structures. In **1**, the carboxylate ndc caused the 2D square-grid (4,4) layers with the paddle-wheel shaped $[Cd_2(CO_2)_4]$ dimer, which are further linked by the bmimb ligands, leading to the formation of a 3D framework with **pcu** topology. And two independent nets interlock each other to form a 3-fold interpenetrating framework. When the rigid bis(imidazole) ligands were introduced into the reaction system, another two 3D frameworks were obtained. In **2**, five **dia** networks interweave to form a 5-fold interpenetrated framework. However, complex **3** shows a 4-connected coordination, non-interpenetrated network with an extremely rare $(6^5\cdot 8)$-**hxg-d**-4-*Cccm* topology. Compared with bip ligand, the bibp ligand has two extra methyl groups on the benzene ring. The electron of benzene ring was changed which may affect the structures of the complexes. Consequently, it is obviously that the linkage of central metal ion, the conformation and linkage orientation of organic ligands have significant effects on the resultant topology of the networks.

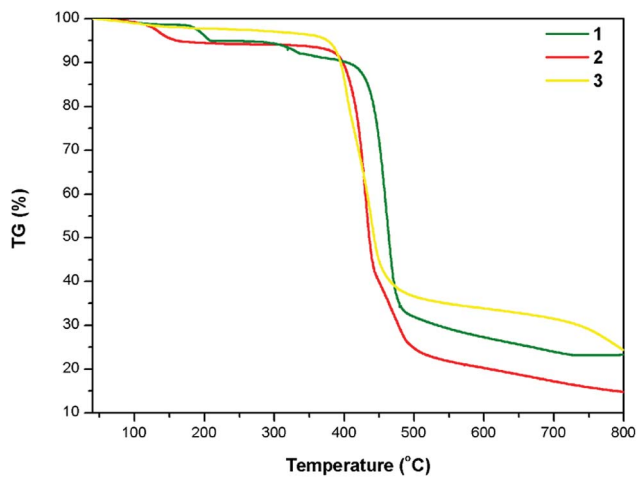

Fig. 4 TGA curves for CPs **1–3**.

3.4. Thermal analysis

The TG analysis was performed in N_2 atmosphere with a heating rate of 10 °C min^{-1} on polycrystalline samples of CPs **1–3**, and the TG curves are shown in Fig. 4. The TG curve of **1** shows an initial weight loss of 5.15% below 230 °C, corresponding to the removal of lattice water molecules (calcd 5.55%). Upon further heating, a second weight loss of 71.09% was observed from 300 to 800 °C, which can be ascribed to the decomposition of organic ligands. The remaining residue corresponds to the formation of CdO (obsd 23.69%, calcd 26.38%). For complex **2**, the first weight loss of 5.48% happened below 200 °C corresponds to the removal of lattice water molecules (calcd 4.79%). The second step weight loss of 81.57% between 300 and 800 °C indicated the decomposition of organic ligands. The remaining weight is assigned to the formation of ZnO (obsd 12.95%, calcd 14.43%). For complex **3**, the first weight loss of 3.67% below 300 °C is consistent with the removal of its lattice water

Table 3 Wavelengths of the emission maxima and excitation (nm) of **1**, **2**, **3**, and organic ligands at room temperature

Complex/ligand	λ_{ex}/nm	λ_{em}/nm
1	323	423
2	300	418
3	300	402
H_2ndc	300	433
bmimp	300	392
bibp	300	382
bip	300	410

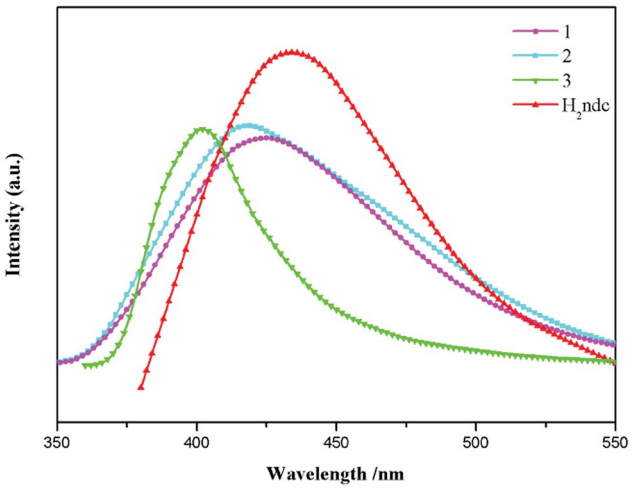

Fig. 5 Photoluminescences of CPs **1–3** at room temperature in solid state.

molecules (calcd 3.57%), and the weight loss of 81.06% from 350 to 800 °C can be ascribed to the release of organic ligands. Upon further heating, the coordinated ligands were lost until the residue was ZnO.

3.5. Photoluminescence properties

Although a lot of transition metal ions have been used to construct CPs, the Zn and Cd-based CPs are the most interested transition-metal-based luminescent CPs. The d^{10} metal ions not only have various coordination numbers and geometries, but also display luminescent properties when coordinated with functional ligands.[26] The coordination polymers are promising candidates for applicable photoluminescent materials such as chemical sensors, light emitting diodes (LEDs), and electrochemical displays and so on.[27] The luminescence properties of complexes **1–3** together with the free H_2ndc, bmimb, bibp, bip ligands, were investigated in the solid state at room temperature (Table 3) and depicted in Fig. 5. The photoluminescent spectra of the free ligands show the main peak at 433 nm (λ_{ex} = 300 nm) for H_2ndc, 392 nm (λ_{ex} = 300 nm) for bmimp, 382 nm (λ_{ex} = 300 nm) for bibp, and 410 nm (λ_{ex} = 300 nm) for bip respectively. The emission spectra for bands were observed at 423 nm (λ_{ex} = 320 nm) for **1**, 418 nm (λ_{ex} = 300 nm) for **2**, and 402 nm (λ_{ex} = 300 nm) for **3**. In comparison to the free ligands, the emission peaks of **1–3** are close to those of the relevant ligands, so the emission bands of these complexes can probably be attributed to the intraligand fluorescence emission. However, the emission maxima of **1–3** are slightly blue-shifted by 10 nm, 15 nm and 31 nm respectively as compared to those of the corresponding the H_2ndc ligand. Considering that Cd(II) and Zn(II) ions are difficult to oxidize or reduce because of their d^{10} configuration, the emission of these complexes are neither metal-to-ligand charge transfer (MLCT) nor ligand-to-metal charge transfer (LMCT) in nature.[28] The photoluminescent of **1–3** may originate from the intraligand π*–π or π*–n transition of the H_2ndc ligand that is modified by the Zn(II) and Cd(II) ions. Different coordination environments may be an important factor on influencing different luminescent behaviours of **1–3**.

4. Conclusions

In summary, three new Zn(II)/Cd(II) CPs constructed from a naphthalene-2,6-dicarboxylic acid and different bidentate imidazole ligand have been successfully obtained by solvothermal method. The X-ray single crystal analysis revealed that these complexes exhibit different supramolecular architectures and the ligands show various coordination sites, modes, as well as conformations. Complex **1** shows a 3-fold interpenetrating 3D network with **pcu** topology. Complex **2** exhibits a 3D 5-fold interpenetrating structure with **dia** topology and complex **3** is a 3D 4-connected coordination network with an extremely rare $(6^5\cdot 8)$-**hxg-d**-4-*Cccm* topology. The structural analysis indicates that the linkage of metal centers, and conformation of organic ligands have important influences on the resulting network topology. Furthermore, the solid-state photoluminescence properties of the CPs at 298 K and thermal stabilities were investigated.

Acknowledgements

This work was supported by the NSFC (Grant nos 21271117, 21371179 and 51372125), NCET-11-0309 and the Fundamental Research Funds for the Central Universities (13CX05010A, 14CX02158A).

References

1 (*a*) L. J. Murray, M. Dinca and J. R. Long, *Chem. Soc. Rev.*, 2009, **38**, 1294; (*b*) H. Uehara, S. Diring, S. Furukawa, Z. Kalay, M. Tsotsalas, M. Nakahama, K. Hirai, M. Kondo, O. Sakata and S. Kitagawa, *J. Am. Chem. Soc.*, 2011, **133**, 11932; (*c*) Y. Kang, F. Wang, J. Zhang and X. Bu, *J. Am. Chem. Soc.*, 2012, **134**, 117881; (*d*) J. R. Li, R. J. Kuppler and H. C. Zhou, *Chem. Soc. Rev.*, 2009, **38**, 1477; (*e*) C. T. He, J. Y. Tian, S. Y. Liu, G. F. Ouyang, J. P. Zhang and X. M. Chen, *Chem. Sci.*, 2013, **4**, 351; (*f*) J. Sculley, D. Yuan and H. C. Zhou, *Energy Environ. Sci.*, 2011, **4**, 2721; (*g*) R. B. Getman, Y. S. Bae, C. E. Wilmer and R. Q. Snurr, *Chem. Rev.*, 2012, **112**, 703.

2 (*a*) Y. J. Cui, Y. F. Yue, G. D. Qian and B. L. Chen, *Chem. Rev.*, 2012, **2**, 703; (*b*) H. Yang, F. Wang, Y. X. Tan, T. H. Li and J. Zhang, *Chem.–Asian J.*, 2012, **7**, 1069; (*c*) M. J. Sie, Y. J. Chang, P. W. Cheng, P. T. Kuo, C. W. Yeh, C. F. Cheng, J. D. Chen and J. C. Wang, *CrystEngComm*, 2012, **14**, 5505; (*d*) G. M. Sun, Y. M. Song, Y. Liu, X. Z. Tian, H. X. Huang, Y. Zhu, Z. J. Yuan, X. F. Feng, M. B. Luo, S. J. Liu, W. Y. Xu and F. Luo, *CrystEngComm*, 2012, **14**, 5714; (*e*) Y. W. Li, H. Ma, Y. Q. Chen, K. H. He, Z. X. Li and X. H. Bu, *Cryst. Growth Des.*, 2012, **12**, 189; (*f*) Z. Y. Du, H. B. Xu and J. G. Mao, *Inorg. Chem.*, 2006, **45**, 9780; (*g*) M. D. Allendorf, C. A. Bauer, R. K. Bhakta and R. J. T. Houk, *Chem. Soc. Rev.*, 2009, **38**, 1330.

3 (*a*) J. Li, J. Tao, R. B. Huang and L. S. Zheng, *Inorg. Chem.*, 2012, **51**, 5988; (*b*) H. L. Wang, D. P. Zhang, D. F. Sun, Y. T. Chen, K. Wang, Z. H. Ni, L. J. Tian and J. Z. Jiang, *CrystEngComm*, 2010, **12**, 1096; (*c*) M. Kurmoo, *Chem. Soc. Rev.*, 2009, **38**, 1353; (*d*) L. H. Jia, R. Y. Li, Z. M. Duan, S. D. Jiang, B. W. Wang, Z. M. Wang and S. Gao, *Inorg. Chem.*, 2011, **50**, 144; (*e*) S. Y. Qian, H. Zhou, A. H. Yuan and Y. Song, *Cryst. Growth Des.*, 2011, **11**, 5676; (*f*) Y. F. Zeng, X. Hu, F. C. Liu and X. H. Bu, *Chem. Soc. Rev.*, 2009, **38**, 469; (*g*) P. Dechambenoit and J. R. Long, *Chem. Soc. Rev.*, 2011, **40**, 3249.

4 (*a*) M. Yoon, R. Srirambalaji and K. Kim, *Chem. Rev.*, 2012, **112**, 1196; (*b*) J. Lee, O. K. Farha, J. Roberts, K. A. Scheidt, S. T. Nguyen and J. T. Hupp, *Chem. Soc. Rev.*, 2009, **38**, 1450; (*c*) M. B. Lalonde, O. K. Farha, K. A. Scheidt and J. T. Hupp, *ACS Catal.*, 2012, **2**, 1550; (*d*) K. S. Jeong, Y. B. Go, S. M. Shin, S. J. Lee, J. Kim, O. M. Yaghi and N. Jeong, *Chem. Sci.*, 2011, **2**, 877; (*e*) L. Q. Ma, C. Abney and W. B. Lin, *Chem. Soc. Rev.*, 2009, **38**, 1248; (*f*) H. Yamazaki, A. Shouji, M. Kajita and M. Yagi, *Coord. Chem. Rev.*, 2010, **254**, 2483.

5 (*a*) G. Férey, *Chem. Soc. Rev.*, 2008, **37**, 191; (*b*) H. X. Zhang, F. Wang, Y. X. Tian, Y. Kang and J. Zhang, *J. Mater. Chem.*, 2012, **22**, 16288; (*c*) J. R. Li, J. Sculley and H. C. Zhou, *Chem. Rev.*, 2012, **112**, 869; (*d*) H. L. Jiang, Y. Tatsu, Z. H. Lu and Q. Xu, *J. Am. Chem. Soc.*, 2010, **132**, 5586.

6 (*a*) M. O'Keeffe and O. M. Yaghi, *Chem. Rev.*, 2012, **112**, 675; (*b*) X. L. Wang, C. Qin, E. B. Wang and Z. M. Su, *Chem.–Eur. J.*, 2006, **12**, 2680; (*c*) I. A. V. Baburin, A. Blatov, L. Carlucci, G. Ciani and D. M. Proserpio, *J. Solid State Chem.*, 2005, **178**, 2452; (*d*) Q. X. Yang, X. Q. Chen, Z. J. Chen, Y. Hao, Y. Z. Li, Q. Y. Lu and H. G. Zheng, *Chem. Commun.*, 2012, **48**, 10016; (*e*) D. Zhao, D. J. Timmons, D. Yuan and H. C. Zhou, *Acc. Chem. Res.*, 2011, **44**, 123.

7 (*a*) X. Zhang, C. Guo, Q. Yang, W. Wang, W. Liu, B. Kang and C. Su, *Chem. Commun.*, 2007, 4242; (*b*) F. L. Hu, W. Wu, P. Liang, Y. Q. Gu, L. G. Zhu, H. Wei and J. P. Lang, *Cryst. Growth Des.*, 2013, **13**, 5050.

8 L. Carlucci, G. Ciani and D. M. Proserpio, *Coord. Chem. Rev.*, 2003, **246**, 247.

9 (*a*) D. M. L. Goodgame, S. A. Menzer, M. Smith and D. J. Williams, *Angew. Chem., Int. Ed. Engl.*, 1995, **34**, 574; (*b*) F. Luo, Y. T. Yang, Y. X. Che and J. M. Zheng, *CrystEngComm*, 2008, **10**, 981; (*c*) Y. Q. Lan, S. L. Li, J. S. Qin, D. Y. Du, X. L. Wang, Z. M. Su and Q. Fu, *Inorg. Chem.*, 2008, **47**, 10600.

10 (*a*) J. Yang, J. F. Ma, S. R. Batten and Z. M. Su, *Chem. Commun.*, 2008, 2233; (*b*) G. H. Wang, Z. G. Li, H. Q. Jia, N. H. Hu and J. W. Xu, *Cryst. Growth Des.*, 2008, **8**, 1932.

11 (*a*) B. Y. Li, F. Yang, Y. M. Zhang, G. H. Li, Q. Zhou, J. Hua, Z. Shi and S. H. Feng, *Dalton Trans.*, 2012, **41**, 2677; (*b*) T. L. Hu, R. Q. Zou, J. R. Li and X. H. Bu, *Dalton Trans.*, 2008, 1302; (*c*) S. S. Chen, J. Fan, T. Okamura, M. S. Chen, Z. Su, W. Y. Sun and N. Ueyama, *Cryst. Growth Des.*, 2010, **10**, 812.

12 Bruker, *SMART, SAINT and SADABS*, Bruker AXS Inc., Madison, Wisconsin, USA, 1998.

13 G. M. Sheldrick, *SHELXS-97, Program for X-ray Crystal Structure Determination*, University of Gottingen, Germany, 1997.

14 G. M. Sheldrick, *SHELXL-97, Program for X-ray Crystal Structure Refinement*, University of Gottingen, Germany, 1997.

15 A. L. Spek, *Implemented as the PLATON Procedure, a Multipurpose Crystallographic Tool*, Utrecht University, Utrecht, The Netherlands, 1998.

16 K. Nakamoto, *Infrared and Raman Spectra of Inorganic and Coordination complexes*, John Wiley & Sons, New York, 1986.

17 A. W. Addison, T. N. Rao, J. Reedijk, J. van Rijn and G. C. Verschoor, *J. Chem. Soc., Dalton Trans.*, 1984, 1349.

18 J.-Q. Liu, Y.-S. Huang, Y.-Y. Zhao and Z.-B. Jia, *Cryst. Growth Des.*, 2010, **11**, 569–574.

19 L. Lin, R. M. Yu, W. B. Yang, X. Y. Wu and C. Z. Lu, *Cryst. Growth Des.*, 2012, **12**, 3304.

20 (*a*) X. L. Zhao, F. Liu, L. L. Zhang, D. Sun, R. M. Wang, Z. F. Ju, D. Q. Yuan and D. F. Sun, *Chem.–Eur. J.*, 2014, **20**, 650; (*b*) D. Sun, M.-Z. Xu, S.-S. Liu, S. Yuan, H.-F. Lu, S.-Y. Feng and D.-F. Sun, *Dalton Trans.*, 2013, **42**, 12326; (*c*) J. Yang, X. Q. Wang, F. N. Dai, L. L. Zhang, R. M. Wang and D. F. Sun, *Inorg. Chem.*, 2014, **53**, 10650; (*d*) X. L. Zhao, J. M. Dou, D. Sun, P. P. Cui, D. F. Sun and Q. Y. Wu, *Dalton Trans.*, 2012, 1928; (*e*) X. Q. Wang, J. Yang, L. L. Zhang, F. L. Liu, F. N. Dai and D. F. Sun, *Inorg. Chem.*, 2014, **53**, 11206–11212.

21 L. Yang, D. R. Powell and R. P. Houser, *Dalton Trans.*, 2007, 955.

22 (*a*) S. S. Chen, Q. Liu, Y. Zhao, R. Qiao, L. Q. Sheng, Z. D. Liu, S. Yang and C. F. Song, *Cryst. Growth Des.*, 2014, **14**, 3727–3741; (*b*) L. Zhou, C. G. Wang, X. F. Zheng, Z. F. Tian, L. L. Wen, H. Qu and D. F. Li, *Dalton Trans.*, 2013, 16375–16386; (*c*) D. Lassig, J. Lincke, R. Gerhardt and H. Krautscheid, *Inorg. Chem.*, 2012, **51**, 6180–6189; (*d*) S. S. Chen, J. Fan, T. Okamura, M. S. Chen, Z. Su, W. Y. Sun and N. Ueyama, *Cryst. Growth Des.*, 2010, **10**, 812–822; (*e*) G. B. Li, J. R. He, M. Pan, H. Y. Deng, J. M. Liu and C. Y. Su, *Dalton Trans.*, 2012, 4626–4633; (*f*) J. H. Park, W. R. Lee, Y. Kim, H. J. Lee, D. W. Ryu, W. J. Phang and C. S. Hong, *Cryst. Growth Des.*, 2014, **14**, 700.

23 (*a*) C. S. Liu, X. G. Yang, M. Hu, M. Du and S. M. Fang, *Chem. Commun.*, 2012, **48**, 7459; (*b*) N. Yuan, T. L. Sheng, J. Zhang, C. B. Tian, S. M. Hu, X. H. Huang, F. Wang and X. T. Wu, *CrystEngComm*, 2011, **13**, 5951.

24 W. Fischer and E. Koch, in *International Tables for Crystallography A*, ed. T. Hahn, Kluwer, Dordrecht, 1983, ch. 14.

25 O. D. Friedrichs, M. O'Keeffe and O. M. Yaghi, *Acta Crystallogr., Sect. A: Found. Crystallogr.*, 2003, **59**, 22.

26 (*a*) J. Y. Zou, H. L. Gao, W. Shi, J. Z. Cui and P. Cheng, *CrystEngComm*, 2013, **15**, 2682; (*b*) Y. J. Cui, Y. F. Yue, G. D. Qian and B. L. Chen, *Chem. Rev.*, 2012, **112**, 1126; (*c*) X. M. Jing, H. Meng, G. H. Li, Y. Yu, Q. S. Huo, M. Eddaoudi and Y. L. Liu, *Cryst. Growth Des.*, 2010, **10**, 3489.

27 (*a*) Y. D. Chen, Y. H. Qin, L. Y. Zhang, L. X. Shi and Z. N. Chen, *Inorg. Chem.*, 2004, **43**, 1197; (*b*) Q. Wu,

M. Esteghamatian, N. X. Hu, Z. Popovic, G. Enright, Y. Tao, M. D'Iorio and S. Wang, *Chem. Mater.*, 2000, **12**, 79; (*c*) G. Li, Z. Lei and Q. M. Wang, *J. Am. Chem. Soc.*, 2010, **132**, 17678.

28 (*a*) H. Y. Liu, H. Wu, J. F. Ma, Y. Y. Liu, B. Liu and J. Yang, *Cryst. Growth Des.*, 2010, **10**, 4795; (*b*) W. Q. Kan, Y. Y. Liu, J. Yang, Y. Y. Liu and J. F. Ma, *CrystEngComm*, 2011, **13**, 4256; (*c*) H. Y. Bai, J. Yang, B. Liu, J. F. Ma, W. Q. Kan and Y. Y. Liu, *CrystEngComm*, 2011, **13**, 5877.